

**Recent Changes in Arctic Ocean Sea Ice Motion  
Associated with the North Atlantic Oscillation**

Ron Kwok

*Jet Propulsion Laboratory  
California Institute of Technology  
4800 Oak Grove Dr  
Pasadena, CA 91109*

*Submitted to Science*

## **Recent Changes in Arctic Ocean Sea Ice Motion Associated with the North Atlantic Oscillation**

Ron Kwok  
Jet Propulsion Laboratory  
California Institute of Technology  
4800 Oak Grove Dr  
Pasadena, CA 91109

**Examination of a new ice motion dataset of the Arctic Ocean over a recent eighteen year period (1978-1996) reveals patterns of variability that can be linked directly to the North Atlantic Oscillation. The intensity of the Icelandic Low, one of its centers of action, modulates the sea level pressure distribution over a broad region of the Arctic Ocean and the Nordic (Greenland-Iceland-Norwegian and Barents) Seas. Over the winters of 1988 through 1995, the Oscillation has remained in its positive phase contributing to coherent large scale changes in the intensity and character of ice transport in the Arctic Ocean. The significant changes include: the spin down of the Beaufort Gyre; the increase in ice export through the Fram Strait; the increase in ice import from the Barents/Kara Seas; the enhanced eastward transport of sea ice from the Laptev Sea; the weakening of the Transpolar Drift Stream; and, the reduction in ice extent in the Nordic Seas. All of these changes affect the regional and total sea ice mass balance of the Arctic Ocean.**

*climate change*

The North Atlantic Oscillation (NAO) is a major source of interannual variability in the atmospheric circulation pattern in the North Atlantic (1) and is most pronounced during winter. It accounts for more than one-third of the total variance in the sea-level pressure (SLP). *Hurrell* (1) defined an index of the NAO as the SLP anomalies between Lisbon, Portugal and Stykkisholmur, Iceland. The positive phase of NAO (NAO+) is characterized by an intense Icelandic low with a strong Azores ridge to its south. This

low affects a broad region of the Arctic Ocean. The signs of these anomalies are reversed in its negative phase (NAO-). Starting in 1988, there has been an upward trend in the NAO index (Fig. 1). Between 1978 and 1987, there are approximately equal number of months (37 vs 40) with  $NAO < -1$  and  $NAO > 1$ . After 1987, there were 40 months with  $NAO > 1$  and only 21 months with  $NAO < -1$ . This is then followed by a dramatic reversal in phase in 1996.

Recently, *Thompson and Wallace* (2) described an Arctic Oscillation (AO) pattern and associated index obtained from the analysis of wintertime SLP records (1958-1997) poleward of  $20^{\circ}\text{N}$  using empirical orthogonal functions. The AO pattern, covering a larger horizontal scale and incorporates many of the features of the NAO, has a mode of the oscillation that involves a seesaw of SLP between the Arctic basin and the surrounding zonal ring. We find a correlation of 0.73 between the DJFM NAO and AO indices between 1978 and 1996. The AO pattern and the 50 mbar height patterns are strongly correlated demonstrating vertical coupling between the lower atmosphere and the strength of the polar vortex. This lends credence to describing these oscillations fundamentally as atmospheric phenomena rather than surface or sea ice events.

Partitioning the SLP (3) and newly-developed ice motion fields (4) based on the NAO index shows distinct shifts in spatial patterns that are associated with the positive and negative phases of NAO (Fig. 2). The difference field (Fig. 3) shows the influence of an intense Icelandic Low (a depression of more than 12 mbar) that imparts an enhanced cyclonic component on atmospheric circulation and sea ice motion, not unlike the two regimes of wind-forced ice circulation proposed by *Proshutinsky and Johnson* (5). During NAO-, there is a well-defined high pressure cell centered over the Beaufort Sea. In contrast, there are no closed isobars over the Arctic Ocean during NAO+. Poleward of  $70^{\circ}\text{N}$ , the extremes of SLP are much lower during NAO- (range: 1020-1008 mbar) than during NAO+ (range: 1015-998 mbar) even though the surface pressure over the central

Arctic is much higher. *Walsh* (6) noted a weakening of the Arctic anticyclone since 1988, most likely a consequence of the dominance of the Icelandic Low during the prevailing NAO+ conditions in the late 1980s and early 1990s. These pressure variations in the Arctic Ocean are also captured in the Arctic Oscillation. Strengthening of the polar vortex results in lower surface pressure. The mean SLP in the central Arctic decreased by almost 5 mbar over the 18-year period between 1978-1995. The Eurasian Low pressure cell centered over the Barents Sea during NAO- is situated further southwest under NAO+ conditions. Intermediate SLP distributions are evident between the two NAO extremes.

These changes in the SLP distributions over the Arctic Ocean have significant impact on sea ice circulation patterns as gradients in SLP are largely responsible for the motion of sea ice. Away from coastal boundaries, the geostrophic wind explains more than 70% of the variance of daily ice motion in the winter and summer (7). Large scale circulation of sea ice determines the advective part of the ice balance. Changes in the circulation patterns affect ice flux, ice extent, ice age and thickness distributions in the Arctic Ocean. During NAO-, the Beaufort Gyre (anticyclonic sea ice circulation pattern) and the Transpolar Drift Stream (TPS) are distinctive features in the mean motion fields (1978-1987) associated with the Beaufort high pressure cell centered within the Canada Basin. The TPS transports sea ice from the north of Siberia and the Beaufort Sea toward Fram Strait. All four fields show flow out of the Laptev Sea, a primary source of ice in the TPS. In contrast, the Beaufort Gyre is not fully formed in the NAO+ motion fields and the TPS has a different character. There is no significant flow parallel to the Siberian coast in the East Siberian Sea. As a result of the enhanced cyclonic component centered near Iceland, sea ice from the Laptev and the Kara is advected further east before being entrained in a much weakened TPS with its axis shifted westward toward the Canada Basin. *Steele and Boyd* (8) suggest this as an indication for the transport of more fresh riverine shelf water from the Kara and Laptev further east before such water flows out

into the deep basins, leading to the retreat of cold halocline layer from the Amundsen into the Makarov Basin in the 1990s.

There is significant correlation ( $R=0.86$ ) between the sea ice area flux and the NAO index over the months of December through March (9). The average winter area flux over the 18-year record (1978-1996) is  $670,000 \text{ km}^2$ , approximately 7% of the area of the Arctic Ocean and ranges from a minimum of  $450,000 \text{ km}^2$  in 1984 to a maximum of  $906,000 \text{ km}^2$  in 1995 (Fig. 4). Over the 18-year record, there is an upward trend in the ice area flux associated with the positive phases of NAO. The SLP gradient across the Fram Strait explains more than 80% of the variance in the area flux, has a correlation with NAO of more than 0.7. The center of the the Icelandic Low, during positive phases of NAO, is positioned in such a manner as to enhance the gradient in the SLP across the Fram Strait by almost 1 mbar thus increasing the atmospheric forcing on ice transport. Correlation is reduced during the negative NAO years because of decreased dominance of this large-scale atmospheric pattern on the cross-strait pressure gradient.

The Fram Strait fresh water flux, transported by sea ice, affects the global thermohaline circulation: a key element of the climate system on decadal (Great Salinity Anomaly) to millennial time-scales (10). If this circulation is disrupted or weakened, the consequences for high-and mid-latitude continental climate are severe (11). Small changes in Fram Strait outflow are thought to affect the delicate balance with respect to the underlying water masses in the Greenland Sea and are sufficient to permit or restrain deep convection. Correlation between five years of volume flux estimates (1991-1995) and the NAO index gives  $R=0.56$ . The average winter volume flux over the winters of Oct 1990 through May 1995 is  $1745 \text{ km}^3$  ranging from a low of  $1375 \text{ km}^3$  in flux to a high of  $2791 \text{ km}^3$  in 1995, varied by a factor of two over the short five year record of NAO+. With this magnitude of variability, the excess fresh water of  $2000 \text{ km}^3$  first observed north of Iceland during

the mid-1960s characterized as the 'Great Salinity Anomaly' can therefore be accounted for by only moderate perturbations of outflow from the Arctic Ocean (12).

Lower correlation of the volume flux with the NAO (relative to the area flux) is plausible because volume flux is dependent on the mean ice thickness of the source regions in addition to the variability in atmospheric forcing. Associated with the changes in the TPS, the outflow through Fram Strait can be seen to come from quite different parts of the Arctic Ocean under different NAO conditions. This suggests that the variability of NAO affects the mean thickness of the ice outflow, regional mass balance and total ice volume of the Arctic Ocean. The regional outflow rate determines the residence time and in turn the regional ice age and ice thickness. The NAO+ motion fields seem to favor source regions in the Eurasian Basin whereas the NAO- motion fields indicate larger contributions of sea ice from the East Siberian Sea and thicker ice from the Beaufort Sea. South of Fram Strait, the ice motion fields also show enhanced transport through the Denmark Strait due to increased pressure gradient associated with NAO+ (Table 2).

The Kara Sea appears to be a net exporter of sea ice, sometimes into the eastern Arctic Ocean and other times into the Barents Sea. Between 1978-1996, the area flux of sea ice through the following passages: Svalbard-Franz Josef Land, Franz Josef Land-Novaya Zemlya and Franz Josef Land-Severnaya Zemlya are shown in Fig. 3. The ice area flux through these passages are small compared to the Fram Strait outflow and all are negatively correlated, with various intensities, to the NAO index (Table 1). The correlation is most likely dependent on the orientation of the passages relative to the cyclonic circulation pattern due to the Icelandic Low. The most significant being the inflow of sea ice from the Barents and Kara Seas through the Franz Josef Land-Severnaya Zemlya passage. There was sustained inflow of sea ice through this passage during the prevailing NAO+ conditions between 1988-1996.

The sea ice extent in the Greenland and Barents Seas is also linked to the NAO. Here, the time series of April ice extent anomalies from satellite passive microwave observations (13) that exhibited a downtrend over the eighteen years, is negatively correlated (-0.64) to the DJFM NAO index. The southerly winds due to the cyclonic circulation pattern tend to push the ice edge northward and westward. This is consistent with the ice motion pattern in these regions (Table 2). During NAO+, the zonal component of ice motion in the East Greenland Sea is toward the Greenland coast thus decreasing the ice extent. The meridional component, however, is enhanced as indicated by the increase in ice area flux discussed above. Under NAO- conditions, the zonal component of ice motion is much higher transporting the ice southward and eastward toward the Greenland Sea. In contrast, the meridional component of ice motion in the Barents Sea is much higher during low NAO. This favors the southward motion of the ice edge increasing ice coverage in the Barents Sea. The NAO+ motion fields also show enhanced southward advection of sea ice in Baffin Bay and Davis Strait (Table 2). Large positive sea ice extent anomalies and negative surface air temperature anomalies in Hudson Bay, Baffin Bay and Labrador Sea during episodes of strong NAO were reported by *Mysak et al.* (14)

The above discussion focused on the linkages between the recent changes in the Arctic Ocean ice motion, ice flux and ice extent and the NAO. Recently, others (15) have reported increased moisture flux into the Arctic, increased ocean transport into the Arctic Ocean through the Barents Sea, and a warming and freshening of Atlantic Water inflow to the Arctic Ocean in the West Spitzbergen Current, all in connection with the increased NAO (North Atlantic Oscillation) index in the late 1980s. Decadal variability in the NAO have become more pronounced since 1950. Prolonged periods with anomalous atmospheric circulation pattern associated with the positive and negative phases of NAO could create irreversible changes of the ice cover of the Arctic Ocean. These coupled ice, ocean and atmospheric interactions link the Arctic climate system to the lower latitudes and are therefore of wide interest in the context of global climate.

## References and Notes

1. J. W. Hurrell, *Science*, 269, 676 (1995).
2. D. W. J. Thompson and J. M. Wallace, *Geophys. Res. Lett.*, in press.
3. The sea level pressure data are provided by the International Arctic Buoy Program.
4. This blended ice motion dataset is created by combining ice motion observations (R. Kwok, R., A. Schweiger, D. A. Rothrock, S. Pang and C. Kottmeier, *J. Geophys. Res.*, 103, 8191 (1998)) from sequential satellite passive microwave fields (37 GHz, 85 GHz) and drifting buoy data in the following manner:  
$$\hat{u} = \sum_i \alpha_i \tilde{u}_i^{85\text{GHz}} + \sum_j \beta_j \tilde{u}_j^{37\text{GHz}} + \sum_k \gamma_k \tilde{u}_k^{\text{buoy}}$$
$$u$$
 is ice motion and  $\alpha$ ,  $\beta$  and  $\gamma$  are weighting coefficients determined by an optimal interpolation procedure.
5. A. Y. Proshutinsky and M. A. Johnson, *J. Geophys. Res.*, 102, 12493 (1997).
6. J. E. Walsh, W. L. Chapman and T. L. Shy, *J. Clim.*, 9, 480 (1996).
7. A. Thorndike and R. Colony, *J. Geophys. Res.*, 87, 5845 (1982).
8. M. Steele and S. Boyd, *J. Geophys. Res.*, 103, 10419 (1998).
9. R. Kwok and D. A. Rothrock, *J. Geophys. Res.*, 104, 5177 (1999).
10. W. S. Broecker, D. M. Peteet and D. Rind, *Nature*, 315, 21 (1985).
11. W. R. Schmitt, *Reviews of Geophysics*, 1395, (1995); S. Manabe and R. J. Stouffer, *J. Climate*, 841, (1988).
12. K. Aagaard and E. Carmack, *J. Geophys. Res.*, 94, 14485 (1989). The fresh water budget lists ice flux through Fram Strait as the largest single component of the Greenland-Iceland-Norwegian (GIN) Sea freshwater balance.
13. The sea ice extent of the Greenland and Barents Seas area provided by J. C. Comiso, Goddard Space Flight Center.
14. L. A. Mysak, R. G. Ingram, J. Wang and A. van der Baaren, *Atmosphere-Ocean*, 35, 333 (1996).



15. R. R. Dickson et al., *J. Climate*, in press; J. Zhang, D. A. Rothrock and M. Steele, *Geophy. Res. Lett.*, 25, 1745 (1998).
16. This work was performed at the Jet Propulsion Laboratory, California Institute of Technology, and was sponsored by the National Aeronautics and Space Administration and the National Oceanic and Atmospheric Administration.

### **Figure Captions**

Figure 1. Winter (December through March) index of the NAO based on the difference of the normalized pressure between Lisbon, Portugal and Stykkisholmur, Iceland (after *Hurrell (1)*). The DJFM NAO indices are averages of their monthly values.

Figure 2. Spatial patterns of monthly (October through May) sea-level pressure and ice motion fields between 1978 and 1996 partitioned based on the NAO index. (a)  $NAO > 1$ . (b)  $0 < NAO \leq 1$ . (c)  $-1 < NAO \leq 0$ . (d)  $NAO \leq -1$ . The contour increment is 1 mbar.

Figure 3. Difference between the  $NAO > 1$  and  $NAO \leq -1$  sea-level pressure and ice motion fields in Fig. 2.

Figure 4. Time series of ice area flux through Fram Strait, Svalbard-Franz Josef Land, Franz Josef Land-Novaya Zemlya, Franz Josef Land - Severnaya Zemlya.

### DJFM NAO index (1978-1996)

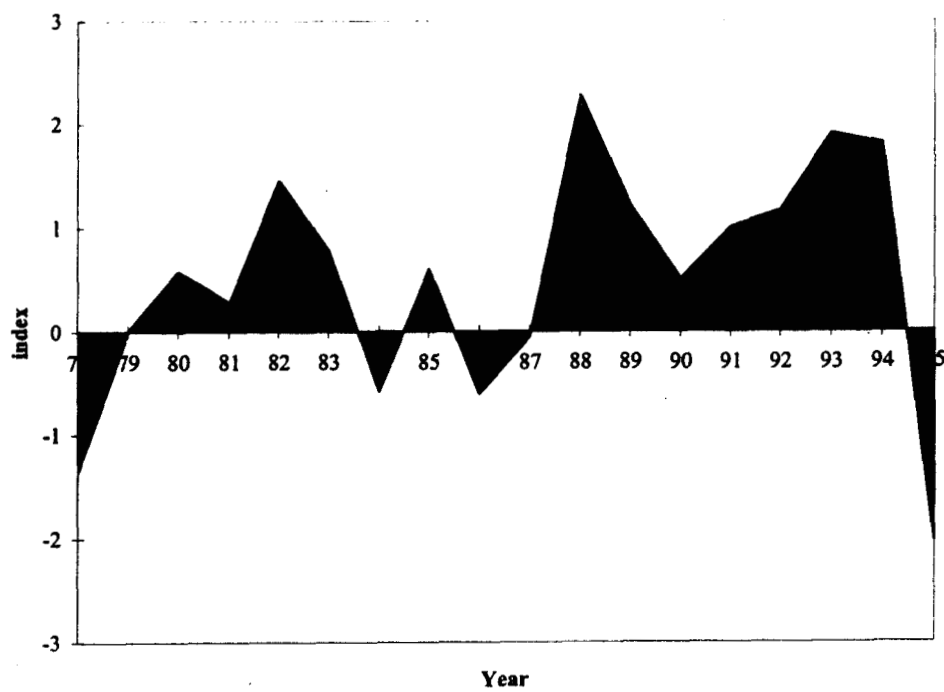
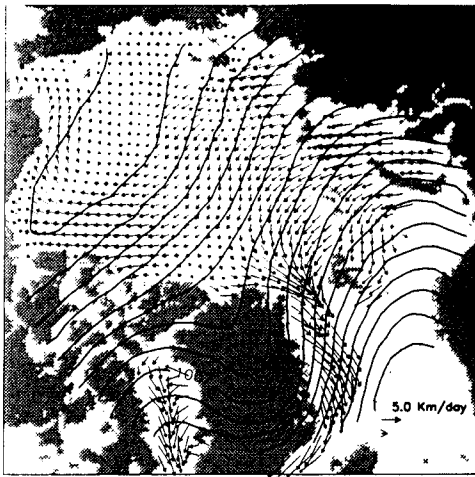
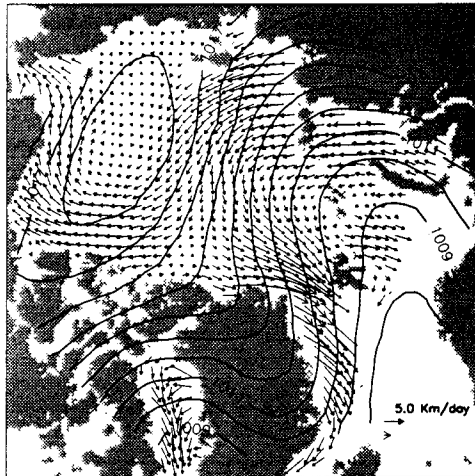


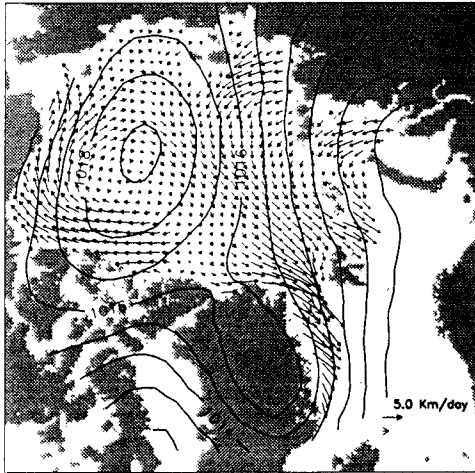
Fig. 1



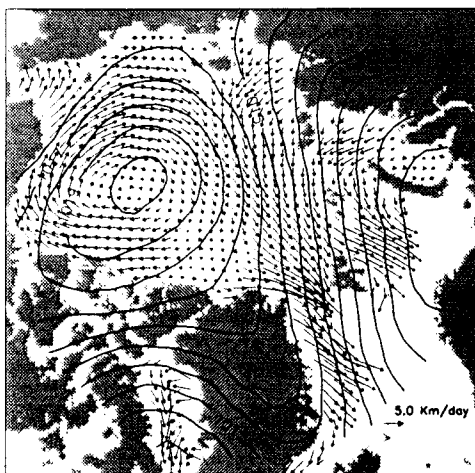
a)  $NAO > 1$



b)  $0 < NAO < 1$



c)  $-1 < NAO < 0$



d)  $NAO < -1$

Difference between  $NAO > 1$  and  $NAO < -1$

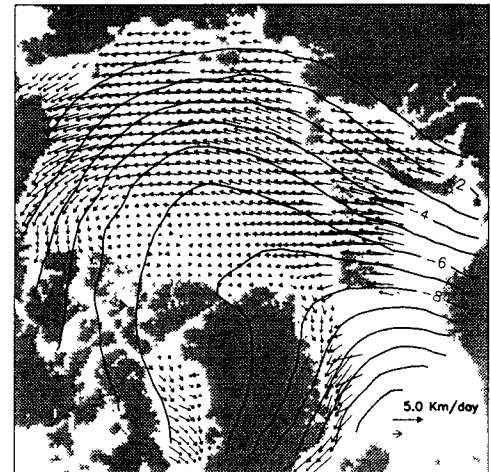


Fig. 3

Fig. 2

### Winter (October-May) Sea Ice Area Flux

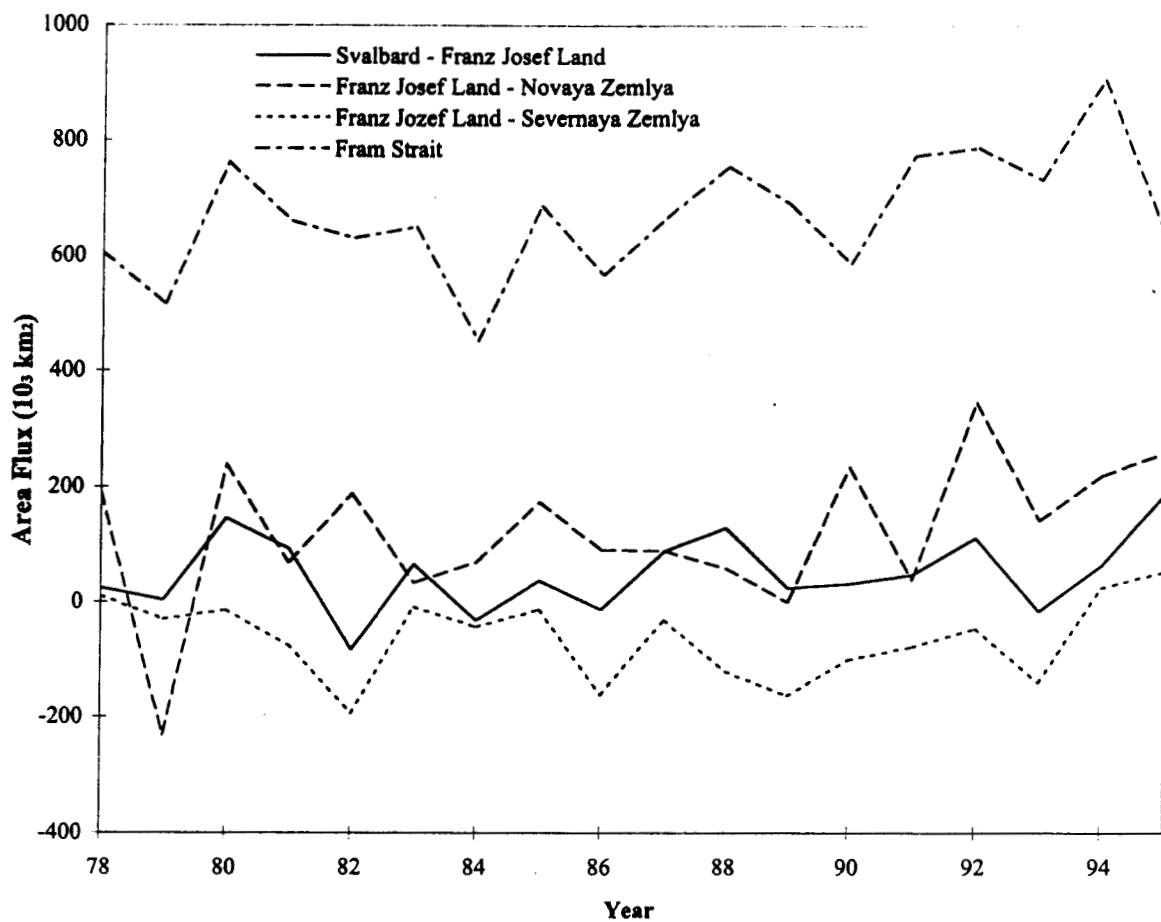


Fig. 4

Table 1  
Arctic Ocean area flux ( $10^3 \text{ km}^2$ ) October through May 1978 - 1996  
(+ indicates outflow)

Flux gate	Avg	Min	Year	Max	Year	Correlation (NAO, Area Flux)
Svalbard - Franz Josef Land	47	-83	1982	187	1995	-0.52
Franz Josef Land - Novaya Zemlya	126	-232	1979	348	1992	-0.17
Franz Josef Land - Severnaya Zemlya	-65	-195	1982	52	1995	-0.74

Table 2  
Partitioning of meridional ( $v_m$ ) and zonal ( $v_z$ ) velocities (cm/s) based on NAO index

Location (lat, lon)	1 < NAO		0 < NAO < 1		-1 < NAO < 0		NAO < -1	
	$v_m$	$v_z$	$v_m$	$v_z$	$v_m$	$v_z$	$v_m$	$v_z$
<i>a) East Greenland Sea</i>								
69N 20W	-7.1	-4.8	-5.3	-3.0	-4.0	-2.8	-3.2	-1.4
72N 16W	-10.1	-3.9	-8.4	-2.7	-6.8	-2.3	-6.1	-0.5
75N 12W	-12.2	-2.6	-10.2	-1.6	-9.0	-1.2	-9.7	-0.1
<i>b) Barents Sea</i>								
78N 35E	-0.9	-4.6	-3.5	-1.2	-3.8	-4.7	-5.9	-4.6
78N 40E	-0.3	-5.0	-3.5	-1.8	-3.4	-5.6	-6.1	-5.5
78N 45E	0.7	-4.7	-2.1	-1.4	-2.0	-5.4	-4.5	-6.1
78N 50E	2.4	-4.2	-0.7	-0.7	-1.2	-3.7	-2.2	-6.0
<i>c) Baffin Bay/Davis Strait</i>								
69N 60W	-10.0	4.0	-8.9	3.1	-6.8	1.4	-7.5	1.9
72N 64W	-8.9	4.2	-7.7	4.2	-7.1	1.5	-7.9	1.9
73N 68W	-8.1	5.7	-7.2	5.2	-5.8	3.2	-6.3	4.1